Proceedings of Czech–Japanese Seminar in Applied Mathematics 2004
August 4-7, 2004, Czech Technical University in Prague
http://geraldine.fjfi.cvut.cz
pp. 128–138

NUMERICAL SIMULATION OF DISLOCATION DYNAMICS BY MEANS OF PARAMETRIC APPROACH

VOJTĚCH MINÁRIK[1] , JAN KRATOCHVÍL[2] , AND KAROL MIKULA[3]

Abstract. The aim of this contribution is to present the current state of our research in the field of numerical simulation of dislocations moving in crystalline materials. The simulation is based on recent theory treating dislocation curves and dipolar loops interacting by means of forces of elastic nature and hindered by the lattice friction. The motion and interaction of one dislocation curve and one or more dipolar loops placed in 3D space is considered. Results of numerical experiments made by parametrical approach to the problem (using flowing finite volume method) are presented and behaviour of the motion is described in detail.

Key words. FDM, flowing finite volume method, method of lines, parametric curves

AMS subject classifications. 35K65, 68U20, 74M25, 74S10

1. Introduction. Plastic deformation of crystalline solids is a result of the motion of dislocations. The theory of dislocations is described in number of text books, e.g. [7]. Here we recall only the basic mobile properties of dislocations and the nature of their mutual interactions.

A dislocation is a line defect of the crystal lattice. Along the dislocation line the regular crystallographic arrangement of atoms is disturbed. The dislocation line is represented by a closed curve or a curve ending at the surface of the crystal. At low homologous temperatures the dislocations can move only along crystallographic planes (the slip planes) with the highest density of atoms. The motion results in mutual slipping of the neighbouring parts of the crystal along the slip planes. The slip displacement carried by a single dislocation, called Burgers vector, is equal to one of the vectors connecting the neighbouring atoms.

The displacement field of atoms from their regular crystallographic positions around a dislocation line can be treated (except the close vicinity of the line) as elastic stress and strain fields. On the other hand, a stress field exerts a force on a dislocation. The combination of these two effects causes the elastic interaction among dislocations.

There are two types of dislocations having much different characteristic length scales and mobile properties: *dislocation curves* and *dipolar loops*. Detailed description of these two types of dislocations can be found in [7] or [12]. The aim of this contribution is not to describe theory of dislocations; we would like to present results of our simulations and to comment them. Readers interested more in mathematical model and more details about the flowing finite volume method may find information in [12].

[1]Department of Mathematics, Faculty of Nuclear Sciences and Physical Engineering, Czech Technical University in Prague, Trojanova 13, 120 00 Praha 2, Czech Republic.
[2]Department of Physics, Faculty of Civil Engineering, Czech Technical University in Prague, Thákurova 7, 166 29 Praha 6, Czech Republic.
[3]Department of Mathematics and Descriptive Geometry, Slovak University of Technology, Radlinského 11, 813 68 Bratislava, Slovakia.

2. Dislocation curve and dipolar loop. We consider a plane dislocation segment with fixed ends; the segment represented by a plane curve can bow in a slip plane which is identified with the xz-plane of the coordinate system, i.e. $y = 0$. If the dislocation segment approaches a loop, the curve can pass by or the curve and the loop start to move together or the curve is stopped by the loop [9].

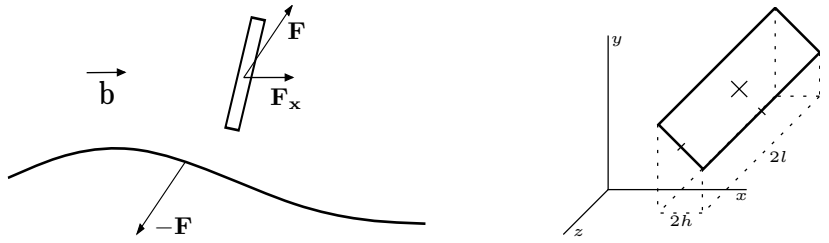

(a) Force interaction (b) DL geometry

FIG. 2.1. *Dislocation dynamics problem geometry: (**a**) Dislocation curve and dipolar loop interaction; (**b**) Dipolar loop geometry*

As the loop is allowed to move along the direction parallel to its Burgers vector $\vec{b}$ only (see Figure 2.1a) just the force component in that direction causes the loop motion. Additionally, the lattice friction acts against the motion. The detailed condition for the dislocation curve and the loop is specified in Section 3.3.

The position of the loop is represented by 3 coordinates of its centre. There are two types of dipolar loops: a *vacancy dipolar loop* and an *interstitial dipolar loop*; each type has two stable configurations [12] with normals $\frac{1}{\sqrt{2}}[1,1,0]$ and $\frac{1}{\sqrt{2}}[1,-1,0]$.

In vacancy loops a strip of atoms in regular crystallographic positions is missing. On the other hand; in interstitial loops an extra strip of atoms is added. For that reason the vacancy and interstitial loops produce different stress fields. The Burgers vectors of vacancy and interstitial loops have opposite directions. This fact we incorporate into our model by using negative value for the x-axis component of the Burgers vector for interstitial loop.

According to [12] dipolar loops are small rectangles denoted V_1, V_2, I_1, and I_2 with longer sides parallel to the z-axis of the coordinate system. Average size of a dipolar loop is denoted by $2l$ and $2\sqrt{2}h$.

3. Mathematical model.

3.1. Interaction of dislocation lines. The interaction force per unit length of dislocation line is given by the Peach-Koehler equation, which written for the i-th component reads

$$f_i = \varepsilon_{ijk}\sigma_{jm}b_m s_k \ , \tag{3.1}$$

where we denote:

f_i	i-th component of the interaction force per unit length of the dislocation line
ε_{ijk}	Levi-Civita symbol
σ_{jm}	components of the stress field tensor at the dislocation position
b_m	components of the Burgers vector
s_k	components of unit tangential vector of the dislocation line

3.2. Stress field of dipolar loop. Stress field produced by a dipolar loop is given by formula presented by Kroupa et al [10, 13, 12] and is very complex, especially

in the closest neighbourhood of the dipolar loop. Under the assumptions that restrict the motion of dislocation curve and dipolar loops in some directions, and the fact the dipolar loop width h is very small comparing to the other sizes, we can simplify the original Kroupa's formula by using Taylor expansion and integration, and obtain an algebraic formula for the stress field of a dipolar loop:

$$\begin{aligned}\sigma_{xy}(x,y,z) = -\frac{\mu h b}{2\pi(1-\nu)}\Bigg\{ &\left[\frac{l-z}{\varrho_-} + \frac{l+z}{\varrho_+}\right]\left[\frac{x \pm y}{(x^2+y^2)^2}\left(\pm x + y - 8\frac{x^2 y}{x^2+y^2}\right)\right] \\ &+ \left[\frac{l-z}{{\varrho_-}^3} + \frac{l+z}{{\varrho_+}^3}\right]\left[\pm\nu + \frac{xy}{(x^2+y^2)^2}\left(y^2 - 3x^2 \mp 4xy\right)\right] \\ &+ \left[\frac{l-z}{{\varrho_-}^5} + \frac{l+z}{{\varrho_+}^5}\right]\left[-\frac{3x^2 y(x \pm y)}{x^2+y^2}\right]\Bigg\}\,,\end{aligned} \tag{3.2}$$

where

$$\varrho_- = \sqrt{x^2+y^2+(l-z)^2}\,, \quad \varrho_+ = \sqrt{x^2+y^2+(l+z)^2}\,, \tag{3.3}$$

μ is shear modulus, ν is the Poisson ratio, and $[x, y, z]$ is the position relative to the centre of dipolar loop. With the upper sign in (3.2) we get the stress formula for the dipolar loops V_1 and I_1, while with the lower sign we get the formula for V_2 and I_2 dipolar loops. Readers more interested in the origin of (3.2) can find detailed information in [12]. The complexity of the stress field is demonstrated in Figure 5.6.

3.3. Governing equations. The dynamics of the system of a dislocation curve and a dipolar loop is governed by a system of two equations describing their motion. The motion law for the dislocation curve Γ_t can be parameterized by a smooth time dependent vector function $\vec{X} : I \times S \to R^2$, i.e., at any time t it is given as the Image$(\vec{X}(.,t)) = \{\vec{X}(u,t), u \in S\}$ where S is a fixed parameterization interval and I is a time interval. For a smooth curve $|\vec{X}_u| > 0$ and for unit arc-length parameterization s, $\mathrm{d}s = |\vec{X}_u|\mathrm{d}u$. Then $\vec{X}_s$ and $\vec{X}_s^{\perp}$ represent unit tangent and normal vectors, respectively. Using the Frenet formulae, the evolution equation can be written in the form of intrinsic diffusion equation [6, 1, 5, 11]

$$B\vec{X}_t = \varepsilon\vec{X}_{ss} + F\vec{X}_s^{\perp} \tag{3.4}$$

for the position vector $\vec{X}$. Drag coefficient B and line tension ε are material constants and F represents external driving forces. If we denote by $X^x(t,s)$ and $X^z(t,s)$ the components of the dislocation curve position vector in the xz-plane, then $\vec{X}_s^{\perp} = [X_s^z, -X_s^x]$. The equation (3.4) is solved numerically to model complicated dislocation curve dynamics.

The motion law of the dipolar loop can be easily obtained from (3.1) where all stress contributions of the whole dislocation curve should be included:

$$F_x^c = \int_{\Gamma_t} \sigma_{xy} b_{curve} n_x \mathrm{d}s\,. \tag{3.5}$$

The term F_x^c is the x-axis component of the total force acting on a dipolar loop, $n_x = X_s^z$ is the x-axis component of the dislocation curve's normal vector. Incorporating lattice friction F_0 depending on material, the equation governing the gliding of the dipolar loop is

$$\frac{\mathrm{d}x(t)}{\mathrm{d}t} = \frac{1}{BP}F_{x,total}(\Gamma_t, x(t))\,, \tag{3.6}$$

where $x(t)$ is the x-axis position of the dipolar loop, $P = 4(l + \sqrt{2}h)$ is the perimeter of the dipolar loop, and

$$F_{x,total}(\Gamma_t, x(t)) = \begin{cases} F_x^c - F_0 & \text{if} \quad F_x^c > F_0 \\ 0 & \text{if} \quad |F_x^c| < F_0 \\ F_x^c + F_0 & \text{if} \quad F_x^c < -F_0 \, . \end{cases} \tag{3.7}$$

4. Numerical scheme. For discretization of the problem described earlier, we use the flowing finite volume method [11] in space and the method of lines [2, 3, 4] in time. Discrete solution is represented by a moving polygon given, at any time t, by plane points $\vec{X}_i, i = 0, ..., M$. The values $\vec{X}_0$ and $\vec{X}_M$ are prescribed in case of fixed ends of the curve. The segments $\left[\vec{X}_{i-1}, \vec{X}_i\right]$ are called flowing finite volumes. We construct also dual volumes $\mathcal{V}_i = \left[\vec{X}_{i-\frac{1}{2}}, \vec{X}_i\right] \cup \left[\vec{X}_i, \vec{X}_{i+\frac{1}{2}}\right]$, $i = 1, .., M-1$, where $\vec{X}_{i-\frac{1}{2}} = \frac{\vec{X}_{i-1}+\vec{X}_i}{2}$ (see Fig. 4.1).

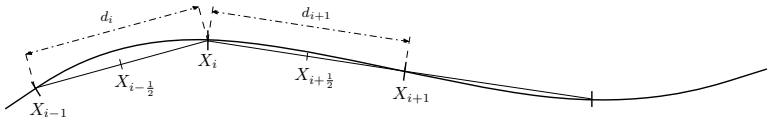

FIG. 4.1. *Piecewise linear approximation of the dislocation curve.*

Integrating evolution equation (3.4) in dual volume $\mathcal{V}_i$ followed by some other straightforward steps described in [12] we get a system of ordinary differential equations:

$$B\frac{\mathrm{d}\vec{X}_i}{\mathrm{d}t} = \varepsilon\frac{2}{d_i + d_{i+1}}\left(\frac{\vec{X}_{i+1} - \vec{X}_i}{d_{i+1}} - \frac{\vec{X}_i - \vec{X}_{i-1}}{d_i}\right) + \frac{2}{d_i + d_{i+1}}F_i\frac{\vec{X}_{i+1}^{\perp} - \vec{X}_{i-1}^{\perp}}{2} \, , \quad i = 1, \ldots, M-1 \, , \tag{4.1}$$

where d_i denote distances between neighbouring nodes of the dislocation curve's discretization.

In discretization of the governing equation (3.5) for the dipolar loop we sum contributions of every curve segment to obtain

$$F_x^c = \sum_{i=0}^{M-1} \sigma_{xy}\left(X_{i+\frac{1}{2}}^x - x(t), -y, X_{i+\frac{1}{2}}^z - z\right) b_{curve}\left(X_{i+1}^z - X_i^z\right) \, , \tag{4.2}$$

where $[x(t), y, z]$ is the centre of the dipolar loop at time t. Next, we use formula (3.7) applied to discrete F_x^c defined above and get

$$\frac{\mathrm{d}x}{\mathrm{d}t} = \frac{1}{BP}F_{x,total}(\vec{X}_0, \ldots, \vec{X}_M, x). \tag{4.3}$$

The complete discrete problem consists of (4.1) and (4.3) with accompanying initial and boundary conditions.

The initial conditions simply describe positions and shapes of the dislocation curve and dipolar loops at the beginning of the computation. As we consider a plane dislocation with fixed ends to model a particular physical process, the boundary condition prescribes positions of the endpoints of the dislocation curve. Thus, no tangential velocity is evaluated for the endpoints.

5. Experimental results.

5.1. Simulation 1 - standalone dislocation curve. In this simulation we present results we got for a standalone dislocation curve exerted to a periodic external stress. Starting with a straight dislocation line fixed at ends, periodic external stress is applied to the system. The dislocation curve allowed to glide only in the xz-plane is either attracted or repelled in the z-axis direction. As positions of the curve end points are fixed, initial straight line becomes curved as the time flows. We observe curvature of the curve (elastic stress of the dislocation) to partly eliminate the external stress, so the curve is not moving with the same speed everywhere. The bigger the curvature is, the slower is the response to the external stress.

Of course, the motion also depends on dimensions of the dislocation curve and the external stress. For a longer curve it takes obviously more time to achieve a higher curvature state (such as a semicircle) than for a shorter curve.

Moreover, if the external stress is not "high enough" (will be precised later), the dislocation curve never transforms to a semicircle. When the external stress is switched off, the curvature pushes the dislocation curve back to its initial position, i.e. straight line. This is in agreement with the well-known *minimal potential energy principle*.

To precise the phrase "external stress is high enough", we should take line tension of the dislocation curve into account. Depending on the ratio of the line tension of the dislocation curve and the external stress, as well as the length of the time period of the external stress, we can get one of the following behaviours:

5.1.1. Behaviour 1 - equilibrium state prior reaching a semicircle shape. If the external stress is small comparing to the line tension of the dislocation curve, the motion stops after a certain time, and the dislocation curve will not reach a semicircle shape. It stops in a position where the external stress and the dislocation curve's line tension are in an equilibrium state. The rest of the time period, before the external stress is decreased or reversed, the dislocation remains in this equilibrium position, no matter how long the time period is (see Figure 5.1 (a)–(d)).

5.1.2. Behaviour 2 - time period of the external stress is too short. If the time period of the external stress is to short, the dislocation curve will not reach the equilibrium state prior the external stress is reversed. After reversing, dislocation curve starts to move backwards, i.e. in the opposite direction it was moving before reversing of the external stress.

5.1.3. Behaviour 3 - external stress is too large. When the external stress is too large and the time period long enough, the dislocation curve will create a so-called Frank-Read source. It blows up through the shape of a semicircle, grows and spreads in a much larger area than was occupied by the semicircle (see Figure 5.1 (e)–(f)).

5.2. Simulation 2 - dislocation curve and one dipolar loop. The second simulation was computed for a single dipolar loop positioned at $[x_0, y_0, z_0]$, while the dislocation curve was again gliding in the xz-plane ($y = 0$). Note the dipolar loop was positioned in a different layer of the atomic lattice than the dislocation curve, i.e. $y_0 \neq 0$.

Two different settings for the external stress were used. In the first one a constant external stress was applied for the whole time of computation, while in the second a periodic external stress was applied. We confirmed several our expectations during the

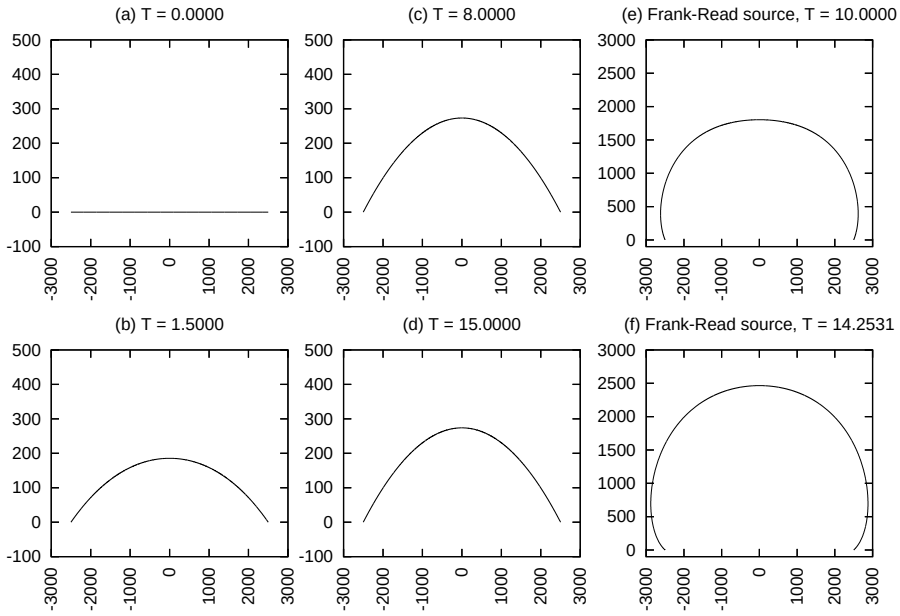

FIG. 5.1. *(a)–(d) Reaching an equilibrium state: at $T \doteq 8$ an equilibrium between the external stress and the line tension of the dislocation curve is reached and remains for the rest of the external stress period; (e)–(f) Creation of Frank-Read source: In the case of large external stress the dislocation curve blows up and a new Frank-Read source is growing further in its neighbourhood*

simulations. The dynamics of the system is highly dependent on the mutual relative position of the dislocation curve and the dipolar loop, on the shape of dislocation curve, and, of course, on the stress applied.

The dipolar loop produces its own stress field that interacts with the dislocation curve. Vice versa, the dislocation curve, as a line dislocation, produces a stress field which interacts with the dipolar loop. Both stress fields are of short-range type, and normally the dislocation curve and the dipolar loop do not interact as they are far enough from each other. However, as the dislocation curve moves according to the applied external stress, it can happen that the dislocation curve moves closer to the dipolar loop and the interaction between them gains more influence over the consequent motion of the system. Typically, the dislocation curve bows around the position of the dipolar loop, and is forcing to move the dipolar loop out of its place as in Figure. 5.2 (d) and 5.5.

On the other hand, the dipolar loop is restricted to move only in the x-axis direction, and there is also some amount of energy needed to exceed in order to start the motion at all. Force corresponding to this minimal energy is called friction force.

5.2.1. Positional dependence. The most significant for the behaviour of the system is the relative position of the dipolar loop and the dislocation curve. One can say there is a distance threshold behind which there is almost no interaction. This threshold depends on the direction in space because of the shape of the dipolar loop.

For the y-axis, if the dipolar loop is positioned in a layer too far from the layer (plane) of the dislocation curve, the interaction is negligible. However, for the other two axes the situation is different. Depending on the external stress and its size, as well as on the line tension of the dislocation curve, there are following possibilities:

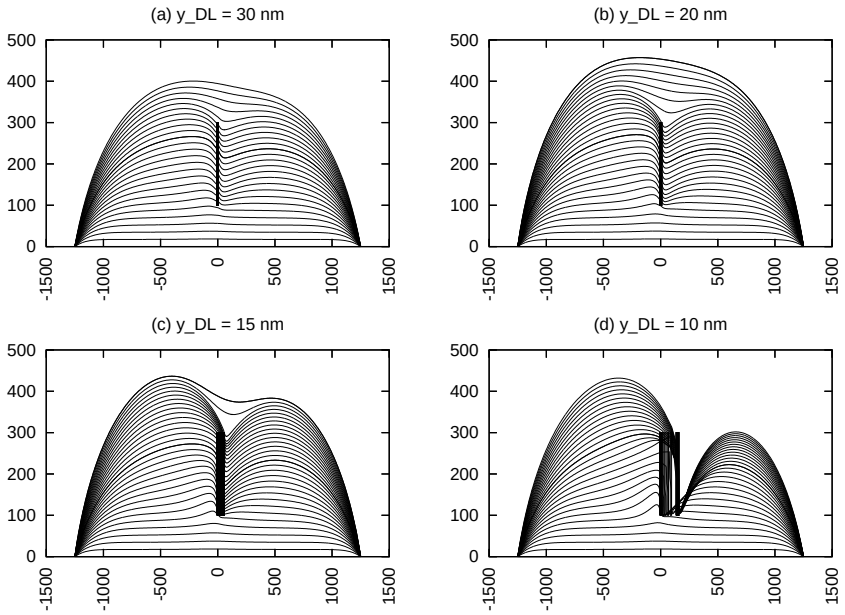

Fig. 5.2. *Dependence on the distance of the dipolar loop layer. Several time levels of the simulation are shown for the dipolar loop positioned initially at* $[0, y_{DL}, 200]$. *For the nearest case where* $y_{DL} = 10$ *nm the dipolar loop sweeps to the right*

- The dislocation curve stops prior to reach the interaction region around the dipolar loop (like in Section 5.1.1). In this case the motion of the dislocation curve is not influenced by the presence of the dipolar loop in the system.
- The dislocation curve is not moving towards the dipolar loop. In this case again the motion of the dislocation curve is not influenced by the presence of the dipolar loop - under the additional assumption both dislocations were not interacting at the beginning of the simulation.
- The dislocation curve is moving (in its glide plane $y = 0$, of course) towards the dipolar loop, and will interact with it at some time of evolution.

5.2.2. Dependence on the shape of the dislocation curve. The dipolar loop can glide out of the dislocation curve's interaction region only if there is a clear way. If, for example, the dipolar loop is surrounded by two hills (see Figure 5.2 (a)) of the dislocation curve, and these two hills are further growing due to the stress applied, the dipolar loop cannot move through the energetic walls of the hills and resides between them. Consequently, the dislocation curve's motion is locally hindered and the curve distorts around the dipolar loop (Figure 5.4). Such a situation is not rare. Even for an initially straight dislocation curve it can happen that the forced motion of the dipolar loop is not fast enough to leave the interaction region. It can be either due to the large friction force (most energy is consumed for overcoming friction, see Figure 5.3), or due to the strong external stress (simply the dislocation curve is moving faster than the dipolar loop can react, see Figure 5.2 (b)).

5.2.3. Dependence on the applied external stress. Consider the situation from one of the previous sections: the dislocation curve is moving towards the dipolar loop. The stronger the external stress is, the closer to can the dislocation curve

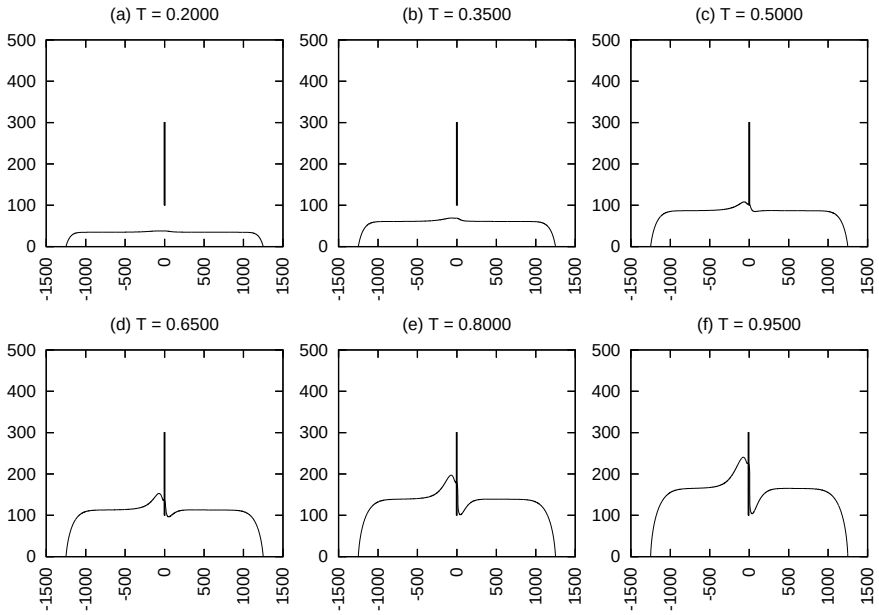

FIG. 5.3. *Dependence on the friction force of the dipolar loop. Several time levels of the simulation are shown for the dipolar loop positioned initially at* $[0, -30, 200]$. *The motion of the dipolar loop is hindered by a large friction*

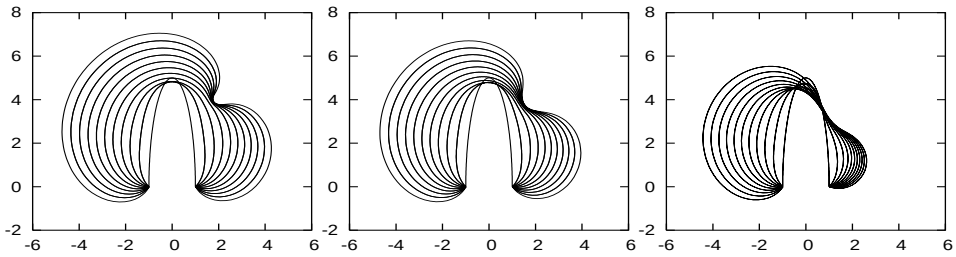

FIG. 5.4. *The dynamics of the system depends on all parameters. The rightmost image uses 4 times bigger dipolar loop than the middle one. The leftmost image uses 2.5 times bigger dipolar loop and 2 times bigger shear modulus than the middle one. Dipolar loop fixed at* $[2, 4, 0.01]$ *is not shown in the images*

approach the dipolar loop. The closer it can approach, the stronger the interaction is. Finally, the stronger is the interaction, the faster the dipolar loop is forced to sweep away (Figure 5.5).

The achieved results seem to be close to the real physical processes in materials. However, during the computations we observed that the dislocation curve bows so fast that the dipolar loops are unable to respond to it. This fact is not in agreement with real physical experiments [8]. We tried to remove this drawback from our model by adding an additional term of elastic relaxation to the governing equation of the dislocation curve. It is a question of further investigations and simulations, how will this term work in the model.

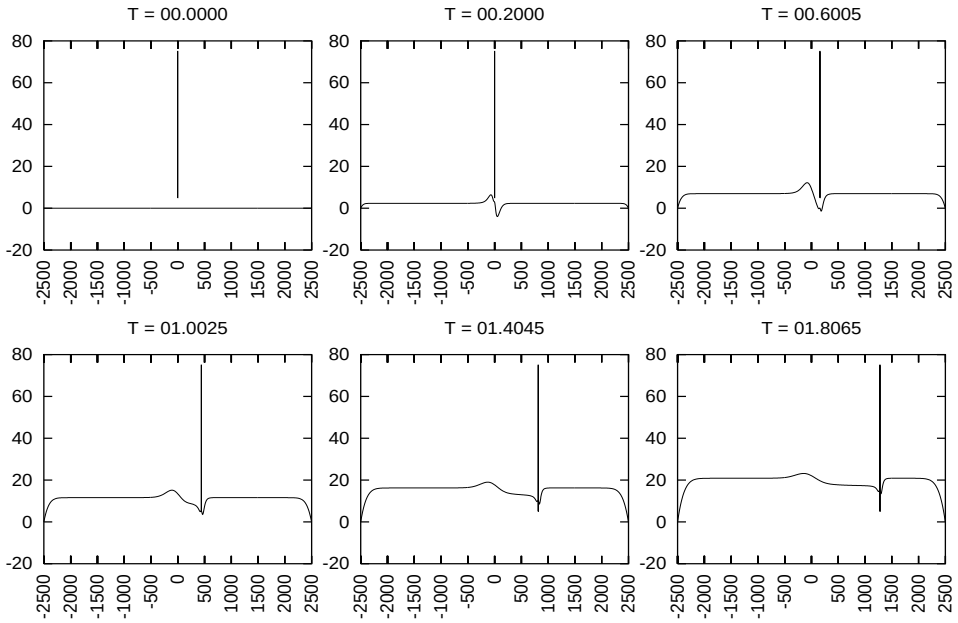

Fig. 5.5. *Dipolar loop swept by the curve; on the other hand, the curve is distorted by the stress field of the loop. In this test there were used:* $\mu = 80$ *GPa,* $\nu = 0.33$*,* $B = 10^{-4}$ *Pa s,* $b = 0.707$ *nm,* $l = 35$ *nm,* $h = \sqrt{2}$ *nm,* $F_0 = 4$ *MPa m, applied stress* $\sigma_a = -1.155$ *MPa. Initial position of dipolar loop was* $[0, 40, -30]$*. The subsequent stages are shown for increasing time* T

Acknowledgements. The first author was partly supported by the NSF grant NSF00-138 Award 0113555 and by the project "Applied Mathematics in Technology and Physics" MSM 6840770010 of the Ministry of Education of the Czech Republic, the second author was partly supported by the project KONTAKT No. ME654 and Grant Agency of the Czech Republic No. 106/03/0826, and the third author was partly supported by the grant VEGA 1/0313/03. The conference participation was possible thanks to the Internal Grant of the Czech Technical University in Prague No. 0415314.

REFERENCES

[1] S.B. Angenent and M.E. Gurtin., *Multiphase Thermomechanics with an Interfacial Structure 2. Evolution of an Isothermal Interface*, Arch. Rat. Mech. Anal., 108 (1989), pp. 323–391

[2] M. Beneš., *Diffuse-Interface Treatment of the Anisotropic Mean-Curvature Flow*, Applications of Mathematics, Vol. 48, No. 6 (2003), pp. 437-453, ISSN 0862-7940

[3] M. Beneš., *Mathematical analysis of phase-field equations with numerically efficient coupling terms*, Interfaces and Free Boundaries 3, (2001), pp. 201–221, ISSN 1463-9963

[4] M. Beneš., *Mathematical and Computational Aspects of Solidification of Crystallic Materials*, Acta Mathematica Universitatis Comenianae, Volume 70 (2001), No. 1, pp. 123–152, ISSN 0862-9544

[5] G. Dziuk., *Convergence of a Semi Discrete Scheme for the Curve Shortening Flow*, Mathematical Models and Methods in Applied Sciences, 4 (1994), pp. 589–606

[6] M. Gage and R.S. Hamilton., *The Heat Equation Shrinking Convex Plane Curves*, J. Diff. Geom., 23 (1986), pp. 69–96

[7] J.P. Hirth and J. Lothe., *Theory of Dislocations*, John Willey (1982)

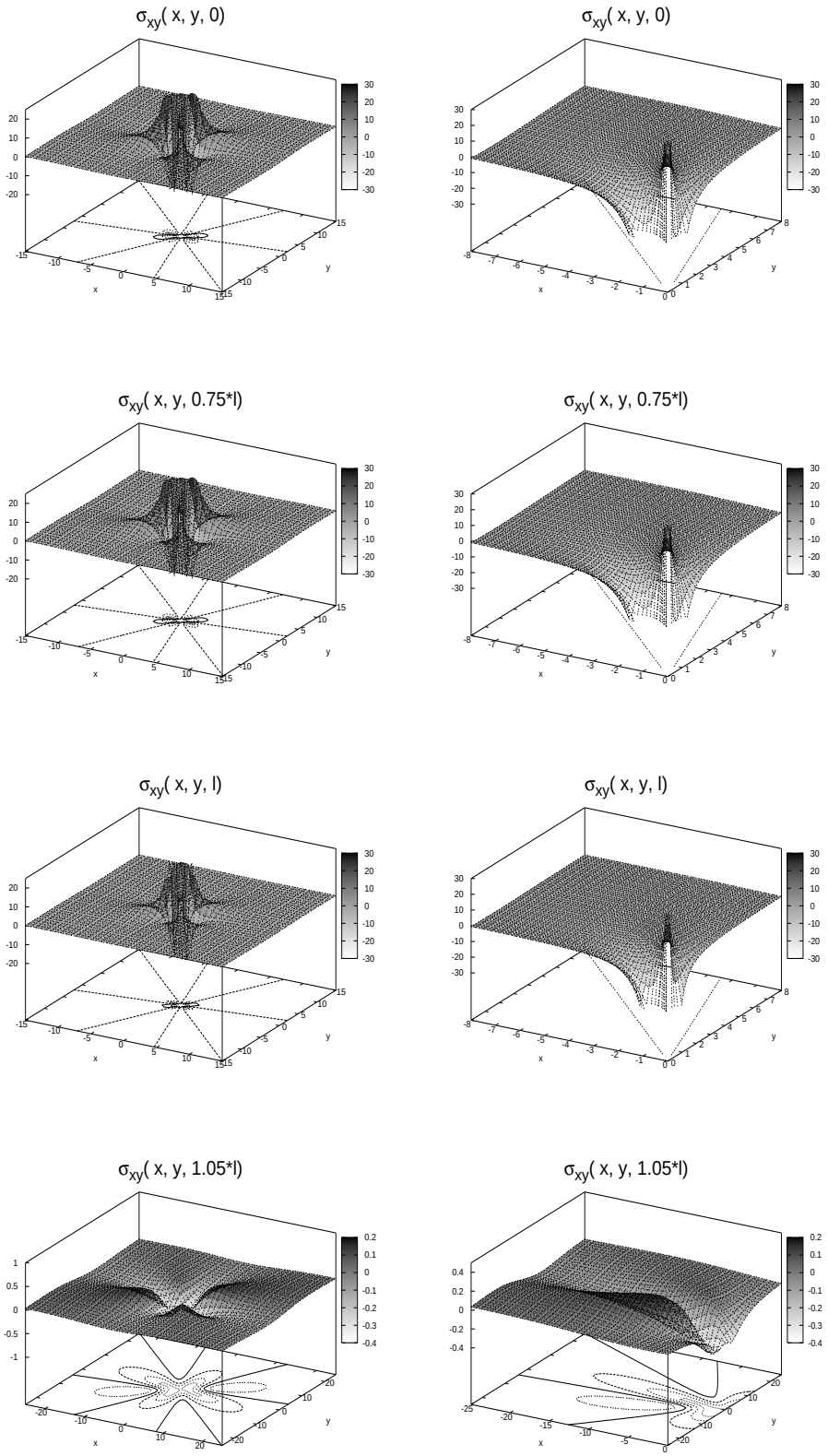

FIG. 5.6. *Complexity of the dipolar loop stress field. Graphs showing stress field at planes* $z = 0$, $z = 0.75l$, $z = l$, *and* $z = 1.05l$ *are presented.*

[8] J. Huang, N.M. Ghoniem and J. Kratochvíl., *On the sweeping mechanism of dipolar dislocation loops under fatigue conditions*, Modelling and Simulation in Materials Science and Engineering, 12 (2004), pp. 917–928

[9] J. Kratochvíl, F. Kroupa and L.P. Kubin., *The Sweeping of Dipolar Loops in Cyclic Deformation: Kinetic Diagrams*, Proceedings of the 20^{th} Risoe Int. Symposium on Material Science: Deformation-Induced Microstructures: Analysis and Relation to Properties. Risoe National Laboratory, Roskilde, Denmark (1999), pp. 387–392

[10] F. Kroupa., *Long-Range Elastic Field of Semi-Infinite Dislocation Dipole and of Dislocation Jog*, phys.stat.sol., Vol. 9 (1965), pp. 27–32

[11] K. Mikula and D. Ševčovič., *Evolution of Plane Curves Driven by a Nonlinear Function of Curvature and Anisotropy*, SIAM J. Appl. Math., Vol. 61, No. 5, pp. 1473–1501

[12] V. Minárik, J. Kratochvíl, K. Mikula and M. Beneš., *Numerical Simulation of Dislocation Dynamics*, Numerical Mathematics and Advanced Applications, ENUMATH (2003), pp. 631–640

[13] Š. Verecký, J. Kratochvíl and F. Kroupa., *The Stress Field of Rectangular Prismatic Dislocation Loops*, Phys. Stat. Sol. (a), Vol. 191 (2002), pp. 418–426